JACS
JOURNAL OF THE AMERICAN CHEMICAL SOCIETY
Article
pubs.acs.org/JACS

Supramolecular Thermo-Electrochemical Cells: Enhanced Thermoelectric Performance by Host–Guest Complexation and Salt-Induced Crystallization

Hongyao Zhou,[†] Teppei Yamada,[*,†,‡,§] and Nobuo Kimizuka[†,‡]

[†]Department of Chemistry and Biochemistry, Graduate School of Engineering, [‡]Center for Molecular Systems, Kyushu University, 744 Motooka, Nishi-ku, Fukuoka 819-0395, Japan

[§]Precursory Research for Embryonic Science and Technology (PRESTO), Japan Science and Technology Agency, 7 Gobancho, Chiyodaku, Tokyo 102-0076, Japan

Supporting Information

ABSTRACT: Thermo-electrochemical cells have potential to generate thermoelectric voltage 1 order higher than that given by semiconductor materials. To overcome the current issues in thermoelectric energy conversion, it is of paramount importance to grow and fulfill the full potential of thermo-electrochemical cells. Here we report a rational supramolecular methodology that yielded the highest Seebeck coefficient of ca. 2.0 mV K^{-1} around ambient temperatures. This is based on the encapsulation of triiodide ions in α-cyclodextrin, whose equilibrium is shifted to the complexation at lower temperatures, whereas it is inverted at elevated temperatures. This temperature-dependent host–guest interaction provides a concentration gradient of redox ion pairs between two electrodes, leading to the eminent performance of the thermo-electrochemical cells. The figure of merit for this system, zT reached a high value of 5×10^{-3}. The introduction of host–guest chemistry to thermoelectric cells thus provides a new perspective in thermoelectric energy conversion.

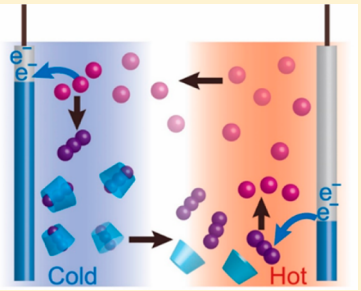

1. INTRODUCTION

Thermo-electrochemical cell (TEC) converts thermal energy into an electrical potential.[1−5] It produces a steady electric current under an applied temperature difference between two electrodes. TECs have been studied for many decades, whose origin dates back to the report by Richards and Nernst in the 19th century.[6] Thermoelectric power induced by a temperature gradient (ΔT) across the material is given by Seebeck coefficient (S_e), defined as $S_e = V_{OC}/\Delta T$, where V_{OC} is thermoelectric open-circuit voltage. It is related to the entropic changes associated with the redox reactions in solution.[7,8]

The power conversion efficiency of thermoelectric materials is represented by a nondimensional figure of merit zT as expressed below:[9−13]

$$zT = \frac{\sigma S_e^{\,2}}{k} T \tag{1}$$

where σ is the electric conductivity, κ is the thermal conductivity, and T is an average temperature of the high- and the low-temperature sides of the cell.[14−16] As expressed in eq 1, the larger S_e value is essential for increasing the zT value.

The key advantages for TEC are their high S_e values which are 1 order of magnitude higher than those reported for the conventional solid thermoelectric alloys such as Bi_2Te_3 (ca. 0.2 mV K^{-1})[17−19] and potentially lower cost.[3,5,20] Since late 1970s, Burrow,[21] Quickenden,[22,23] and Ikeshoji[24] started to study the TEC which uses an aqueous solution of hexacyanoferrate (II/III), and a high S_e value of −1.4 mV K^{-1} was reported. Recently, Baughman,[25,26] Cola,[27] and Kim[20] enhanced the performance of TEC by employing carbon nanotube in electrodes or electrolytes. Pringle and co-workers, meanwhile, reported a TEC using an organic solution of cobalt complex, which showed S_e value of 1.9 mV K^{-1}.[28−30] However, the past studies on TECs have focused on the exploratory search for the better combination of redox pairs and solvents.[7,31−33] It remains a formidable challenge to develop new and rational methodologies that prominently enhance the S_e value.

We report herein the concept of supramolecular TECs that harnesses host–guest inclusion phenomena to control local concentration of electroactive species, which leads to significant improvement of the cell performance. We employed cyclodextrins (CDs) in this study because of their pronounced inclusion phenomena in aqueous environment.[34] α-CD is a six-membered ring of glucose units, which are connected by α-1,4-glycosidic bonds. The inner cavity of α-CD is hydrophobic and shows inclusion phenomena for hydrophobic guest molecules. CDs have been widely employed in many disciplines including the synthesis of supramolecular interlocked molecules,[35,36] molecular assemblies,[37,38] molecular separations,[39] electrochemical[40] and fluorescence sensors,[41] hydrogels,[42,43] and drug delivery sytems.[44] Although CDs have been also utilized to complexate redox active molecules such as ferrocene,[45−47]

Received: May 12, 2016
Published: August 10, 2016

DOI: 10.1021/jacs.6b04923
J. Am. Chem. Soc. 2016, 138, 10502−10507

polyoxomethalates,[38] and iodine,[37] no investigations were made in the field of TECs.

According to the Nernst equation, an equilibrium potential of a half-cell is related to the balance of chemical activities of oxidants and reductants.[48,49] When one of the redox species is selectively captured by CDs to be redox-inert, the relative concentration of the uncaptured species increases. As the association constant of guests to CDs normally decreases with increase of temperature, a concentration gradient of the free guest species is created in the working TEC. It is expected to lead the emergence of extra voltage in TECs, which will increase the S_e value accordingly.

As a redox-active guest molecule, we selected triiodide (I_3^-) because α-CD exhibits efficient host−guest inclusion phenomena with this moderately hydrophobic anion.[50−52] A schematic illustration of the present supramolecular TEC is shown in Figure 1. Two electrodes are in contact to electrolytes at high

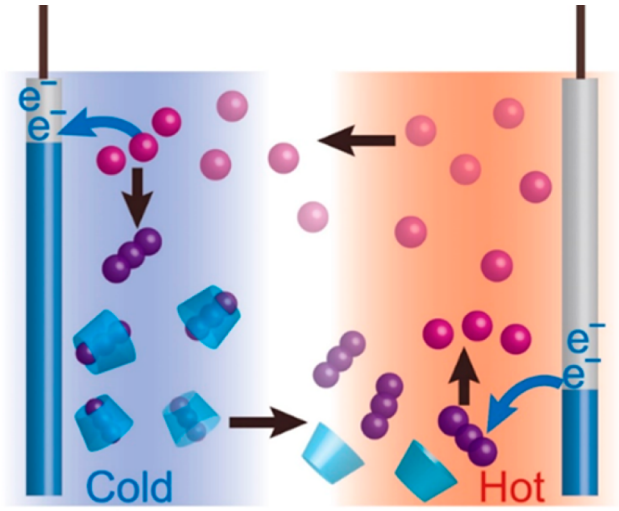

Figure 1. A schematic figure of supramolecular TEC in the combination of α-CD and I_3^-/I^- redox pair.

and low temperatures. The encapsulation of I_3^- by α-CD is promoted at the lower temperature side, which reduces the relative concentration of redox-active I_3^- species. Consequently, the equilibrium shift occurs toward the oxidation of $3I^-$ to produce I_3^- in the cold-electrode side. Meanwhile, dissociation of the α-CD−I_3^- complex is expected to be promoted at elevated temperature, which increases the relative concentration of free I_3^- and then the equilibrium shifts toward the reduction of I_3^- to $3I^-$. By introducing the host−guest interactions, we observed 70% increase in the S_e. Interestingly, when potassium chloride (KCl) was further added to the α-CD−I_3^-/I^- system, an additional open-circuit voltage was generated to the cell, leading to the highest S_e of ca. 2.0 mV K^{-1}. It involved huge decrease in the concentration of free I_3^- anions as a result of the salt-induced segregation of solid K[α-CD_2−I_5] complexes at the cold electrode side. These observations clearly indicate that host−guest chemistry boosts the thermoelectric performance of TEC. Furthermore, the added KCl serves as supporting electrolytes, contributing to increase the ionic conductivity of the electrolyte solution. Since redox ions carry electrons in TECs, the enhanced ionic conductivity σ in eq 1 leads to the increase in zT value. As a result, we obtained zT value of 5×10^{-3}. Together with the theoretical analysis, it is established that a host−guest interaction plays a crucial role to enhance the S_e and the thermoelectric performance of TECs.

2. EXPERIMENTAL SECTION

2.1. Electrolyte Solution of KI_3/KI and α-CD. KI (415 mg, 2.50 mmol) and I_2 (317 mg, 1.25 mmol) were dissolved into water (25 mL) to produce an aqueous solution **1** (KI_3 = KI = 50 mM). Aqueous solutions of **1** (2.5 mL), α-CD (25 mM, 0−10 mL), and KI (100 mM, 3.75 mL) were messed up to 50 mL to produce a solution **2** (KI = 10 mM; KI_3 = 2.5 mM; α-CD = 0−5 mM). KCl (746 mg, 10.0 mmol) was added in each solution **2** to produce solutions **3** (KCl = 200 mM), respectively.

2.2. Thermoelectric Voltage and Current Measurements. Solutions **2** or **3** prepared above (40 mL) were put into an H-shape glass tube (Figure S1). The hot and the cold electrode sides were put into two water bath at different temperature. The electrolyte solution was stirred during the measurement. The temperature inside the cell were monitored by thermometer (TM201, AS ONE, Japan). The cold-side temperature was always kept at approximately 10 °C. Platinum wires were soaked with concentrated sulfuric acid and rinsed with water before used as electrodes. The surface area of the Pt wire was calculated to be 0.47 cm^2. Voltage and current were measured by Sourcemeter, KEITHLEY 2401, after those values became stable.

2.3. Isothermal Titration Calorimetry (ITC). Association constants were evaluated by ITC at 10, 25, 40, and 55 °C. VP-ITC 2000L was used in the experiment. The calorimeter was calibrated by water−water measurement before use. Aqueous solution of I_3^-/I^- (3.5 mM) was put into the syringe and that of α-CD (0.30 mM) was loaded in the cell (1.4 mL). Deionized water was loaded instead of α-CD solution in a baseline measurement. Ten μL of I_3^-/I^- solution was injected into the cell every 3 min. The injection was carried out 20 times in total. The final ΔH graph was obtained by subtracting the baseline, and data of the first injection were removed as an irrelevant one (Figure S2). Association constant was estimated from the gradient of the fitting curve at I_3^-/α-CD = 1. The fitting was carried out by Origin (ver. 5 SR2, OriginLab) and iterated until its χ^2 value reached the minimum.

2.4. UV−vis Spectroscopy. An electrolyte solution of α-CD, I_3^-, and KCl (5 mL) in the hot/cold side was centrifuged (MX205, TOMY SEIKO, Japan) for 10 min at 10,000 rpm. The centrifuging temperature was set at the same as the cell temperature (min. 5 °C, Max. 35 °C). The centrifuged electrolyte was skimmed and diluted in 6% with water. Spectra of the solutions were measured in the 1 mm quartz cell by UV−vis spectrophotometric analyzer (V670, JASCO, Japan).

2.5. Single-Crystal XRD Analysis. Single-crystal XRD analysis was executed with Rigaku VariMax diffractometer with graphite-monochromated MoKα radiation (λ = 0.71070 Å). A crystal of K[α-CD_2−I_5] was mounted onto a goniometer, and the diffraction data were collected with Saturn 724+ CCD detector and processed using Crystal Clear software package. Structure were estimated by direct method and refined with SIR-2004 and Shelx 2014, respectively, on Yadokari software package.

2.6. Ionic Conductivity. Ionic conductivity of the electrolyte solutions is measured by portable electric conductivity meter (ES-71, HORIBA Scientific, Japan). The temperature of the samples (100 mL) are kept at 25 ± 1 °C by soaking in a water bath. Precipitations in the sample (when KCl is added) were removed by filtration before measurement.

3. RESULTS AND DISCUSSION

3.1. Encapsulation of I_3^- by Cyclodextrin and an Improvement in the Thermoelectric Voltage and Seebeck Coefficient. The performance of aqueous I_3^-/I^- TEC (concentration: KI_3 = 2.5 mM, KI = 10 mM) was first investigated without CDs. Figure 2 shows dependence of the open-circuit voltage (V_{OC}) of the TEC on the temperature difference (ΔT) between two electrodes. V_{OC} of the cell

DOI: 10.1021/jacs.6b04923
J. Am. Chem. Soc. 2016, 138, 10502−10507

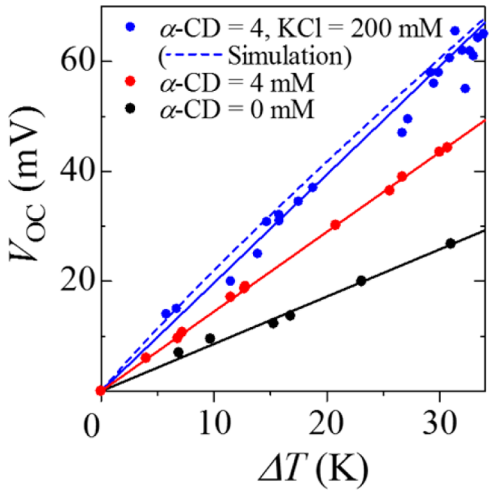

Figure 2. Linear increase of V_{OC} with ΔT in I_3^-/I^- TEC. The base electrolyte is an aqueous solution of KI_3 = 2.5 mM and KI = 10 mM. The slope of lines represents the Seebeck coefficients (S_e); S_e = 0.86 ± 0.02 mV K^{-1} for the pristine I_3^-/I^- cell (black solid circle); S_e = 1.45 ± 0.04 mV K^{-1} for the I_3^-/I^- cell with α-CD (4 mM) (red solid circle); S_e = 1.97 ± 0.09 mV K^{-1} for the I_3^-/I^- cell with α-CD (4 mM) and potassium chloride (200 mM) (blue solid circle), attached with simulation curve.

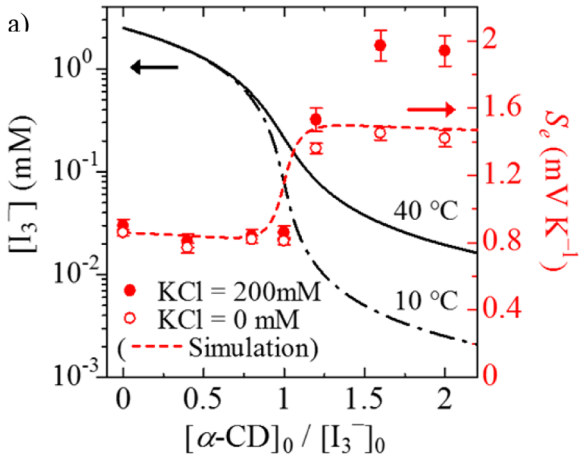

Figure 3. Estimated concentration of uncomplexated I_3^- in the electrolyte solution ($[I_3^-]$) at 10/40 °C and simulated increase of Seebeck coefficient (S_e). $[\alpha\text{-CD}]_0$ = 0–5 mM, $[KI_3]_0$ = 2.5 mM, $[KI]_0$ = 10 mM.

increased linearly with elevating ΔT, and the Seebeck coefficient (S_e) determined from the slope of lines is 0.86 mV K^{-1} (Figure 2). This value is slightly higher than the reported value[1] of 0.53 mV K^{-1}, probably due to the lower temperature and concentration of redox species employed, which affected their chemical activities. The observed enhanced voltage generation in the I_3^-/I^- system is reasonably explainable by thermodynamics; three I^- ions are liberated by the reduction of one I_3^- molecule, which increases the total entropy of the system and accordingly the reduction is preferred at higher temperature. Meanwhile, when α-CD (4 mM) was added to the solution of I_3^- and I^-, an increase in S_e up to 1.45 mV K^{-1} was observed (Figure 2). As Baughman[26] and Macfarlane[1,28,30] reported, the S_e value of TECs shows dependence on the concentration of the redox couples. We therefore investigated the effect of triiodide concentration without CD (Figure S3). As a result, the S_e of I_3^-/I^- TEC showed a decrease from 0.9 mV K^{-1} (KI_3 = 2.5 mM) to 0.7 mV K^{-1} (KI_3 = 0.03 mM), indicating that lower total concentration of I_3^- causes decrease of the S_e of I_3^-/I^- TEC. It indicates that the temperature-dependent inclusion of I_3^- ions by CD plays crucial role, as will be discussed below.

Temperature dependence of the association constant K_{as} was evaluated from ITC. The results are shown in Table S1. The obtained K_{as} decreases with increasing temperature, which meets the required condition for the supramolecular TEC. The dependence of S_e on the initial relative molecular concentration of α-CD and I_3^- is shown in Figure 3 (S_e was evaluated from Figure S4). Interestingly, the S_e value showed a drastic increase at the equimolar concentration of α-CD and I_3^- to reach the plateau value at 1.4 mV K^{-1}. The complexation of redox-active molecules in the cavity of CD has been reported to prevent electrochemical reactions,[53] and it is reasonable that I_3^- species encapsulated in α-CDs show lower or no electrochemical activity. The temperature-dependent complexation of I_3^- species by α-CD thus provides a reasonable account for the observed increase in the S_e of I_3^-/I^- TEC.

3.2. Enhanced Seebeck Coefficient by Means of Salt-Induced Segregation of CD-I_3^- Complexes. The S_e in the present supramolecular TEC can be improved by further decrement of I_3^- concentrations through the selective precipitation of CD–I_3^- complexes under higher salt concentrations. When KCl was added to the aqueous mixture of α-CD and I_3^-/I^-, needle-shaped single crystals were obtained. This crystal is formed by the 2:1 adduct of α-CD and I_5^- as determined by single-crystal XRD experiment (Figure S5). The structure is basically identical with those reported for α-CD_2–I_5^- complexes containing cadmium counterion.[37,54] It indicates that the addition of potassium cation shielded the electrostatic repulsion between α-CD–I_3^- complexes, promoting the transformation into linearly aligned K[α-CD_2–I_5] complexes and their crystallization.

A solubility product (K_{sp}) of solid K[α-CD_2–I_5] complexes was evaluated from the absorbance of dissolved α-CD–I_3^- complexes at 353 nm (ε = 2.0 × 10^4 M^{-1} cm^{-1}, Figures S6–8).[50,52] While the I_3^- ion is efficiently encapsulated in K[α-CD_2–I_5] complexes at lower temperatures, I_3^- ions are liberated from CDs at higher temperatures because the complex becomes soluble. Remarkably, the S_e increases to a record-high value of 1.97 mV K^{-1} under the presence of solid K[α-CD_2–I_5] complexes. The dependence of S_e on the concentration of α-CD also shows a sharp increase at equimolar concentration of α-CD and I_3^- (Figure 3) and reaches a plateau value. In order to prove that the concentration of I_3^- dominated the increase in S_e, we conducted a theoretical analysis on α-CD–I_3^-/I^- system (Figure S9).

3.3. Theoretical Analysis on the α-CD–I_3^-/I^- Supramolecular TEC. The equilibriums for the formation of α-CD_2–I_5^- complex are described as follows:

$$\alpha\text{-CD} + I_3^- \rightleftarrows \alpha\text{-CD}{-}I_3^-$$

$$K^+ + 2(\alpha\text{-CD}{-}I_3^-) \rightleftarrows K[\alpha\text{-}CD_2{-}I_5] + I^-$$

The ITC experiment confirmed that the addition of potassium chloride exerts little influence on the association constant between α-CD and I_3^- (Figure S10, SI). As described above, the KCl-induced aggregation of α-CD–I_3^- complexes gives solid K[α-CD_2–I_5] from which I^- ions are liberated. The segregation (precipitation) of K[α-CD_2–I_5] significantly

DOI: 10.1021/jacs.6b04923
J. Am. Chem. Soc. 2016, 138, 10502–10507

decrease the concentration of free I_3^- ions in the colder half-cell. As a result, the concentration gap of I_3^- ions between the lower-temperature and higher-temperature half-cells is significantly enhanced, thus leading to the observed remarkable increase in V_{OC} and S_e values.

The S_e for the redox couple of I_3^-/I^- in TEC is expressed as eq 2 (see the discussion on theoretical calculations for Seebeck coefficient of I_3^-/I^- TECs with added cyclodextrins, SI):

$$S_e = \frac{\Delta E_f}{\Delta T} + \frac{R}{2F\Delta T}\left(T_H \ln \frac{[I_3^-]_H}{[I^-]_0^3} - T_C \ln \frac{[I_3^-]_C}{[I^-]_0^3}\right) \quad (2)$$

where the subscripts "H" and "C" represent the corresponding variables for hot/cold sides of cells in an equilibrium, the subscript zero represents an initial state, respectively, and ΔE_f is the difference of formal potential, which relates to activity coefficients of redox species (see SI). The little increase in S_e of pristine I_3^-/I^- TEC after the addition of 200 mM of potassium chloride (from 0.86 to 0.90 mV K^{-1}) without CDs can be ascribed to the changes in the activity coefficient and ΔE_f of I_3^-/I^- redox pair.

In a condition where all α-CD$-I_3^-$ complexes are dissolved, the concentration of uncaptured I_3^- anion ($[I_3^-]$) can be calculated from a quadratic equation (details of the calculation is shown in SI) as shown in eq 3:

$$[I_3^-] = \frac{1}{2}([I_3^-]_0 - [CD]_0 - K_{as}^{-1} + \sqrt{([I_3^-]_0 + [CD]_0 + K_{as}^{-1})^2 - 4[I_3^-]_0[CD]_0}) \quad (3)$$

Apparently, the concentration of uncaptured I_3^- in the system is related to association constant K_{as} and the initial concentrations of α-CD ($[CD]_0$) and I_3^- ($[I_3^-]_0$). Simulation curves for $[I_3^-]$ from eq 3 at 10 and 40 °C are shown in Figure 3. A clear discrepancy in the concentration of I_3^- at 10 and 40 °C appears at $[\alpha\text{-CD}]_0 = [I_3^-]_0$. The theoretical S_e value simulated by eq 2 shows good agreement with the experimental data. Meanwhile, when the aggregation occurs to form α-$CD_2-I_5^-$, the concentration of uncaptured I_3^- anion in the system can be approximated by eq 4 (details of the calculation is shown in SI):

$$[I_3^-] = \frac{\sqrt{K_{sp}[I^-]_0}}{K_{as}([\alpha\text{-CD}]_0 - [I_3^-]_0)} \quad (4)$$

The solubility product (K_{sp}) of solid K[α-CD_2-I_5] was evaluated under the condition; $[\alpha\text{-CD}]_0$ = 4 mM; $[I_3^-]_0$ = 2.5 mM; $[I^-]_0$ = 10 mM (see SI). The theoretical increase of *VOC* in the presence of K[α-CD_2-I_5] is estimated from $V_{OC} = S_e\Delta T$, by applying eqs 2 and 4. The simulated line is indicated in Figure 2, which shows satisfactory agreement with the experimental data.

3.4. Ionic Conductivity and *zT* Value in α-CD$-I_3^-/I^-$ System Supplied with Potassium Chloride As Supporting Electrolyte. Ionic conductivity of the TEC influences the *zT* value as expressed in eq 1. The investigation on the ionic conductivity with increasing the concentration of host molecules is essential for evaluating the performance of supramolecular TECs. Black line in Figure 4a shows the ionic conductivity (σ) obtained for aqueous solution of KI_3/KI ($[KI_3]_0$ = 2.5 mM and $[KI]_0$ = 10 mM) at varied α-CD concentration ($[\alpha\text{-CD}]_0$ = 0–5 mM). Although the encapsulation of I_3^- species by α-CDs could decrease the mobility of I_3^-, the conductivity showed only a little decrease at higher α-CD concentration. This is because potassium and iodide ions are abundantly present in the solution. As a result, under the conditions of $[\alpha\text{-CD}]_0 > [I_3^-]_0$, the power factor ($\sigma S_e^2$) of the TEC increases by three times because of the 70% increment in S_e values.

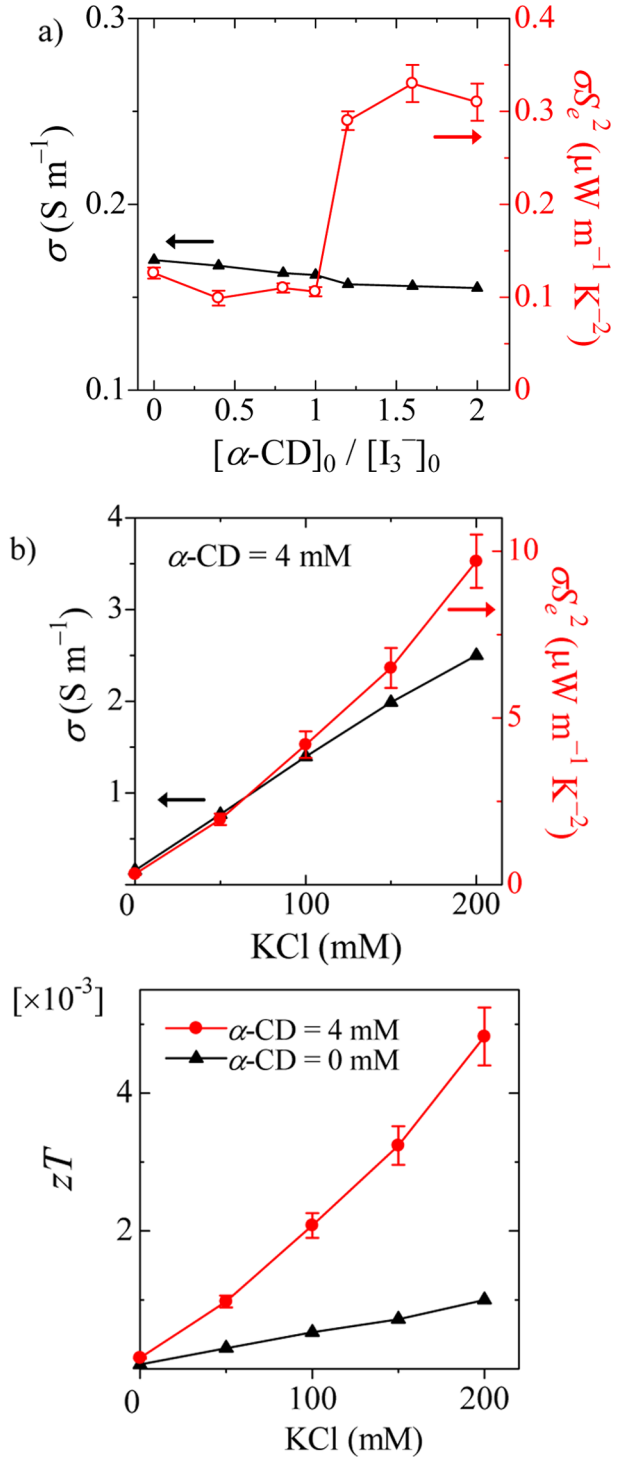

Figure 4. (a) Ionic conductivity (σ) and power factor (σS_e^2) of the electrolyte solution. (b) Increase of ionic conductivity (σ) and power factor (σS_e^2) of the TEC with α-CD (4 mM). (c) Theoretical figure of merit (zT) after the addition of α-CD.

DOI: 10.1021/jacs.6b04923
J. Am. Chem. Soc. 2016, 138, 10502–10507

In order to increase σ in TEC, a straightforward approach is to increase the concentration of redox species.[26,28] However, in this supramolecular system, higher host concentration would be required to encapsulate the guest molecules, and a decrease in the conductivity may become non-negligible. On the other hand, the addition of supporting electrolytes does not affect the host−guest interaction nor redox reaction. In addition, we observed a remarkable synergistic effect that KCl induced transformation and segregation of α-CD−I_3^- complexes that enhanced the S_e at the same time.

Black line in Figure 4a indicates that conductivity of aqueous KI_3/KI with α-CD linearly increases with the concentration of KCl, with no effect of added α-CD (σ and σS_e^2 values without α-CD shown in Figure S11). As we have discussed already, KCl not only serves as the supporting electrolyte, however, it also induces crystallization of α-CD−I_3^- complexes. This effect lead to the nonlinear increase of σS_e^2 as shown in Figure 4a.

As the host α-CDs in the employed low concentration range (0−5 mM) exerted negligible influence on the thermal conductivity (κ) in the solution, we use values of aqueous potassium chloride reported by Ramires and Castro (0.6 W m^{-1} K^{-1} at 300 K, their data plotted in Figure S12, SI).[55] Then zT value of 5×10^{-3} was calculated for α-CD−I_3^-/I^- TEC with 200 mM of potassium chloride (Figure 4b), which is five times higher than the TEC without α-CDs.

3.5. Power Output and Thermal Efficiency of α-CD−I_3^-/I^- TEC. Actual power output of α-CD−I_3^-/I^- TEC was further investigated to calculate the empirical thermal efficiency. We measured the current output while applying external voltage (V) in the opposite direction to the electromotive force of the TEC. The current output was increased at higher concentration of KCl (Figure 5a). This indicates that migration current is a major source of the overall current in TEC. That is, potassium cations and chloride anions migrate between the electrodes to balance the static electric field generated by the redox reaction.

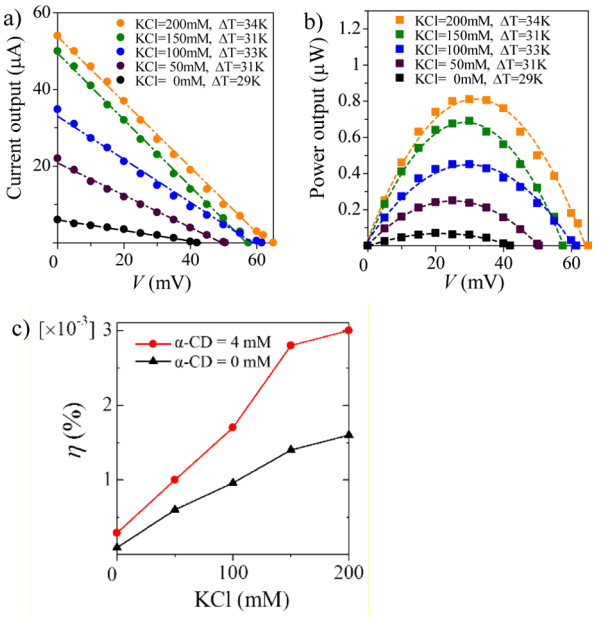

Figure 5. (a) Current output and (b) power output of the TEC with α-CD. ΔT is indicated in the graphs (29−34 K). (c) Empirical thermal efficiency η of the TEC evaluated from the maximum power and an estimated heat flow. The base electrolyte is an aqueous solution of KI_3 = 2.5 mM and KI = 10 mM.

Power output is expressed as the product of the current output and the external voltage (V), and the results are shown in Figure 5b. The maximum power output appears at the half value of V_{OC} because of the linear decrease of the current output. Under the assumption that all of the heat transfers from the hot half-cell to the cold half-cell without thermal loss to ambient air, the heat flux (q) can be calculated as 1.9×10^2 W m^{-2} at ΔT = 30 K (see SI). Then the empirical thermal efficiency (η) is calculated as follows:

$$\eta = \frac{P_{Max}}{qA} \tag{5}$$

where P_{Max} is the maximum power output in Figure 5b, and A is the cross-sectional area of the electrolyte solution in the connecting area between the hot and cold half-cells. The value of η is calculated to be 0.003% when α-CD (4 mM) is added (Figure 5c). This value is higher by a factor of 2 compared to those of pristine I_3^-/I^- TEC at the equal concentration (KI_3 = 2.5 mM, KI = 10 mM) of the redox species. Those results clearly demonstrate the superiority of supramolecular TEC versus conventional one. The output power is mantained for more than 12 h without KCl; however degradation of the power was observed for TEC with an addition of KCl (Figure S13) due to the deposition of precipitate onto the electrode.

4. CONCLUSIONS

A supramolecular TEC has been developed and reported for the first time. This is based on the temperature-dependent inclusion of one species in the redox pair (I_3^-) to the host molecules (cyclodextrin). Since the formation of inclusion complex is promoted in the lower temperature half-cell as compared to that in the higher temperature cell, a concentration gap of redox species created. This gives a rise to an additional thermoelectric voltage and a remarkable increase in Seebeck coefficients. This supramolecular TEC also showed improvement in the power conversion efficiency. All the experimental observations were supported by theoretical analyses, establishing that the host−guest chemistry boosts the development of TECs. Together with the ease in preparation and the use of inexpensive materials, supramolecular TECs would be advantageous for the future real-world applications.

■ ASSOCIATED CONTENT

Supporting Information

The Supporting Information is available free of charge on the ACS Publications website at DOI: 10.1021/jacs.6b04923.

Calculations supporting our theory, description of the TEC used in this study, crystal structure of K[α-CD_2−I_5] and detailed experimental information (PDF)

Crystallographic data (CIF)

■ AUTHOR INFORMATION

Corresponding Author

*teppei@mail.cstm.kyushu-u.ac.jp

Notes

The authors declare no competing financial interest.

DOI: 10.1021/jacs.6b04923
J. Am. Chem. Soc. 2016, 138, 10502−10507

■ ACKNOWLEDGMENTS

This work was supported by PRESTO from JST. This work was supported by Grants-in-Aids for Scientific Research [26708007, 26600026, 24108718] from MEXT. We are grateful to Dr. Yu Hoshino (Department of Chemical Engineering, Graduate School of Engineering, Kyushu University) for the support of ITC measurement. We would like to show our appreciation to Ms. Chihoko Fukakusa for experimental support in thermo-electrochemical cell measurements.

■ REFERENCES

(1) Abraham, T. J.; MacFarlane, D. R.; Pringle, J. M. *Chem. Commun.* **2011**, *47*, 6260.
(2) Chum, H. L.; Osteryoung, R. A. Review of Thermally Regenerative Electrochemical Systems. *U.S. DOE Report SERI/TR-332-416*; DOE: Washington, D.C., 1980; Vol. *1*.
(3) Chang, W. B.; Evans, C. M.; Popere, B. C.; Russ, B. M.; Liu, J.; Newman, J.; Segalman, R. A. *ACS Macro Lett.* **2016**, *5*, 94.
(4) Lee, S. W.; Yang, Y.; Lee, H.-W.; Ghasemi, H.; Kraemer, D.; Chen, G.; Cui, Y. *Nat. Commun.* **2014**, *5*, 3942.
(5) Quickenden, T. I.; Mua, Y. *J. Electrochem. Soc.* **1995**, *142*, 3985.
(6) Richards, T. W. *Z. Phys. Chem.* **1897**, *24*, 39.
(7) Hupp, J.; Weaver, M. *Inorg. Chem.* **1984**, *23*, 3639.
(8) Anari, E. H. B.; Romano, M.; Teh, W. X.; Black, J. J.; Jiang, E.; Chen, J.; To, T. Q.; Panchompoo, J.; Aldous, L. *Chem. Commun.* **2016**, *52*, 745.
(9) Tritt, T. M. *Science* **1999**, *283*, 804.
(10) Disalvo, F. J. *Science* **1999**, *285*, 703.
(11) Slack, G. A.; Hussain, M. A. *J. Appl. Phys.* **1991**, *70*, 2694.
(12) Slack, G. A.; Tsoukala, V. G. *J. Appl. Phys.* **1994**, *76*, 1665.
(13) Hicks, L. D.; Dresselhaus, M. S. *Phys. Rev. B: Condens. Matter Mater. Phys.* **1993**, *47*, 12727.
(14) Snyder, G. J.; Toberer, E. S. *Nat. Mater.* **2008**, *7*, 105.
(15) Bubnova, O.; Khan, Z. U.; Malti, A.; Braun, S.; Fahlman, M.; Berggren, M.; Crispin, X. *Nat. Mater.* **2011**, *10*, 429.
(16) Biswas, K.; He, J.; Blum, I.; Wu, C.-I.; Hogan, T.; Seidman, D.; Dravid, V.; Kanatzidis, M. G. *Nature* **2012**, *489*, 414.
(17) Poudel, B.; Hao, Q.; Ma, Y.; Lan, Y.; Minnich, A.; Yu, B.; Yan, X.; Wang, D.; Muto, A.; Vashaee, D.; Chen, X.; Liu, J.; Dresselhaus, M.; Chen, G.; Ren, Z. *Science* **2008**, *320*, 634.
(18) Rogacheva, E. I.; Grigorov, S. N.; Nashchekina, O. N.; Lyubchenko, S.; Dresselhaus, M. S. *Appl. Phys. Lett.* **2003**, *82*, 2628.
(19) Zhao, X. B.; Ji, X. H.; Zhang, Y. H.; Zhu, T. J.; Tu, J. P.; Zhang, X. B. *Appl. Phys. Lett.* **2005**, *86*, 062111.
(20) Im, H.; Kim, T.; Song, H.; Choi, J.; Park, J. S.; Ovalle-Robles, R.; Yang, H. D.; Kihm, K. D.; Baughman, R. H.; Lee, H. H.; Kang, T. J.; Kim, Y. H. *Nat. Commun.* **2016**, *7*, 10600.
(21) Burrows, B. *J. Electrochem. Soc.* **1976**, *123*, 154.
(22) Quickenden, T. I.; Vernon, C. F. *Sol. Energy* **1986**, *36*, 63.
(23) Mua, Y.; Quickenden. *J. Electrochem. Soc.* **1996**, *143*, 2558.
(24) Ikeshoji, T. *Bull. Chem. Soc. Jpn.* **1987**, *60*, 1505.
(25) Hu, R.; Cola, B. A.; Haram, N.; Barisci, J. N.; Lee, S.; Stoughton, S.; Wallace, G.; Too, C.; Thomas, M.; Gestos, A.; dela Cruz, M. E.; Ferraris, J. P.; Zakhidov, A. a.; Baughman, R. H. *Nano Lett.* **2010**, *10*, 838.
(26) Kang, T. J.; Fang, S.; Kozlov, M. E.; Haines, C. S.; Li, N.; Kim, Y. H.; Chen, Y.; Baughman, R. H. *Adv. Funct. Mater.* **2012**, *22*, 477.
(27) Salazar, P. F.; Stephens, S. T.; Kazim, A. H.; Pringle, J. M.; Cola, B. a. *J. Mater. Chem. A* **2014**, *2*, 20676.
(28) Abraham, T. J.; MacFarlane, D. R.; Pringle, J. M. *Energy Environ. Sci.* **2013**, *6*, 2639.
(29) Abraham, T.; Tachikawa, N.; Macfarlane, D.; Pringle, J. *Phys. Chem. Chem. Phys.* **2014**, *16*, 2527.
(30) Lazar, M. A.; Al-Masri, D.; MacFarlane, D. R.; Pringle, J. M. *Phys. Chem. Chem. Phys.* **2016**, *18*, 1404.
(31) Sahami, S.; Weaver, M. J. *J. Electroanal. Chem. Interfacial Electrochem.* **1981**, *122*, 155.
(32) Yee, E. L.; Cave, R. J.; Guyer, K. L.; Tyma, P. D.; Weaver, M. J. *J. Am. Chem. Soc.* **1979**, *101*, 1131.
(33) Sahami, S.; Weaver, M. J. *J. Electroanal. Chem. Interfacial Electrochem.* **1981**, *122*, 171.
(34) Crini, G. *Chem. Rev.* **2014**, *114*, 10940.
(35) Harada, A. *Acc. Chem. Res.* **2001**, *34*, 456.
(36) Zhao, Y.-L.; Dichtel, W. R.; Trabolsi, A.; Saha, S.; Aprahamian, I.; Stoddart, J. F. *J. Am. Chem. Soc.* **2008**, *130* (34), 11294.
(37) Noltemeyer, M.; Saenger, W. *Nature* **1976**, *259*, 629.
(38) Wu, Y.; Shi, R.; Wu, Y.-L.; Holcroft, J. M.; Liu, Z.; Frasconi, M.; Wasielewski, M. R.; Li, H.; Stoddart, J. F. *J. Am. Chem. Soc.* **2015**, *137*, 4111.
(39) Alsbaiee, A.; Smith, B. J.; Xiao, L.; Ling, Y.; Helbling, D. E.; Dichtel, W. R. *Nature* **2016**, *529*, 190.
(40) Casas-Solvas, J. M.; Ortiz-Salmerón, E.; Fernμndez, I.; García-Fuentes, L.; Santoyo-Gonzμlez, F.; Vargas-Berenguel, A. *Chem. - Eur. J.* **2009**, *15*, 8146.
(41) Hamasaki, K.; Ikeda, H.; Nakamura, A.; Ueno, A.; Toda, F.; Iwao, S.; Osa, T. *J. Am. Chem. Soc.* **1993**, *115*, 5035.
(42) Okumura, Y.; Ito, K. *Adv. Mater.* **2001**, *13*, 485.
(43) Harada, A.; Takashima, Y.; Nakahata, M. *Acc. Chem. Res.* **2014**, *47*, 2128.
(44) Zhang, J.; Ma, P. X. *Adv. Drug Delivery Rev.* **2013**, *65*, 1215.
(45) Kaifer, A. E. *Acc. Chem. Res.* **1999**, *32*, 62.
(46) Nakahata, M.; Takashima, Y.; Hashidzume, A.; Harada, A. *Angew. Chem., Int. Ed.* **2013**, *52*, 5731.
(47) Peng, L.; Feng, A.; Huo, M.; Yuan, J. *Chem. Commun.* **2014**, *50*, 13005.
(48) Mesmer, R. E.; Baes, C. F. J.; Sweeton, F. H. *J. Phys. Chem.* **1970**, *74*, 1937.
(49) Kuzminskii, Y. V.; Zasukha, V. A.; Kuzminskaya, G. Y. *J. Power Sources* **1994**, *52*, 231.
(50) Ramette, R. W.; Sandford, R. W. *J. Am. Chem. Soc.* **1965**, *87*, 5001.
(51) Diard, J. P.; Saint-Aman, E.; Serve, D. *J. Electroanal. Chem. Interfacial Electrochem.* **1985**, *189*, 113.
(52) Minns, J. W.; Khan, A. *J. Phys. Chem. A* **2002**, *106*, 6421.
(53) Matsue, T.; Evans, D.; Osa, T.; Kobayashi, N. *J. Am. Chem. Soc.* **1985**, *107*, 3411.
(54) Noltemeyer, M.; Saenger, W. *J. Am. Chem. Soc.* **1980**, *102*, 2710.
(55) Ramires, M. L. V; Nieto de Castro, C. A. *Int. J. Thermophys.* **2000**, *21*, 671.

DOI: 10.1021/jacs.6b04923
J. Am. Chem. Soc. 2016, 138, 10502−10507